Plasmonics (2015) 10:1657–1662
DOI 10.1007/s11468-015-9980-8

Extraordinary Optical Transmission Exhibited by Surface Plasmon Polaritons in a Double-Layer Wire Grid Polarizer

Atsushi Motogaito[1,2] · **Yuuta Morishita**[1] · **Hideto Miyake**[1,2] · **Kazumasa Hiramatsu**[1,2]

Received: 26 February 2015 / Accepted: 8 May 2015 / Published online: 26 May 2015

Abstract We fabricate a double-layer wire grid polarizer (WGP) and perform optical characterization to clarify the relationship between the structural and polarization characteristics. For normal incidence, the fabricated double-layer WGP exhibits an extinction ratio of 30.4 dB for a period of 400 nm. The transverse magnetic transmittance peak angle is found to vary with the period of the WGP. The peak shift can be explained on the basis of the extraordinary optical transmittance phenomena exhibited by the surface plasmon polaritons (SPPs) of metal slit structures according to the dispersion curve of the SPP. From the simulation of rigorous coupled-wave analysis, it is considered that the incident light passes through the resist layer, followed by the excitation of SPPs at the interface between the resist and Au. Subsequently, the SPPs combine with the transmitted light in the glass substrate, leading to strong transmitted light with transverse magnetic polarization. Therefore, we demonstrate the extraordinary optical transmittance phenomena exhibited by the SPPs by both experiment and simulation.

Keywords Wire grid polarizer · Polarization property · Surface plasmon polariton · Extraordinary optical transmittance phenomena

✉ Atsushi Motogaito
motogaito@elec.mie-u.ac.jp

[1] Graduate School of Engineering, Mie University, Tsu, Mie, Japan

[2] The Center of Ultimate Technology on nano-Electronics, Mie University, Tsu, Mie, Japan

Introduction

A wire grid polarizer (WGP) is a filter-type polarizer. In this study, we investigate the WGP. A WGP is a grating structure arranged by periodic fine metallic patterning. The free electrons can move easily in the direction of the line pattern but are unable to move in the direction perpendicular to the line pattern. Thus, the transverse magnetic (TM) and the transverse electric (TE) light can easily be separated by optical anisotropy. In the 1960s, WGPs operating in the infrared region were fabricated [1–3]. Since the 1990s, WGPs for the visible region have been fabricated with nanostructures using electron beam lithography (EBL) [4–9]. Wang and coworkers fabricated WGPs by using narrow strips less than 100 nm that could be used over a large range of wavelengths, such as the deep UV to near infrared light [9]. The advantages of WGPs compared with the prism-type polarizers are that they are thin and flat structures and able to cover a wider range of incident angle; however, the polarization character of WGPs, such as extinction ratio, is inferior to that of prism-type polarizers. By using these WGP structures, wave plates, such as azimuthal or radial polarization converters, were developed [10–12]. Recently, subwavelength structures or surface plasmon polariton (SPP) have been used to improve the polarization characters [13, 14].

Given these advantages, in this study, we used a double-layer WGP that uses a double layer of metal wire to realize a high optical extinction ratio when compared with a conventional WGP. Furthermore, the double-layer WGP offers the advantage of simplifying the fabrication by eliminating the process of removing the resist. Z. Yu and coworkers fabricated the double-layer WGP and obtained a higher

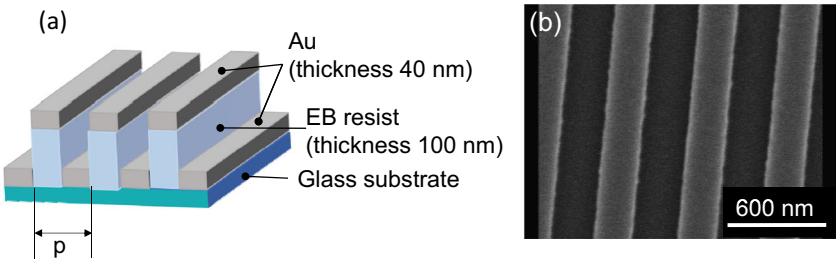

Fig. 1 Schematic of the double-layer WGP made on a glass substrate (**a**), surface morphology of the double-layer WGP, as observed using SEM (**b**)

extinction ratio compared with the conventional single-layer WGP [15]. There are two reasons for the high extinction ratio exhibited by the double-layer WGP, the Fabry–Perot interference and the surface plasmon resonance. Ekinci and coworkers explained that the Fabry–Perot interference and near-field coupling occurred in the double-layer WGP by simulation and experiment [16]. Z. Ye et al. simulated the surface plasmon resonance in the double-layer WGP [17]. They also fabricated a color filter using bilayer metallic nanowire grating or nanowire arrays [18, 19]. There has been theoretical speculation concerning the double-layer WGP in these references, but surface plasmon resonance still has not been confirmed in the double-layer WGP experimentally. Furthermore, Ebbesen et al. showed extraordinary optical transmission using periodic Ag subwavelength hole arrays [20]. This phenomenon can be explained by the surface plasmon resonance combining with the transmitted light. Related studies on the extraordinary optical transmission using SPPs have already been performed [21, 22]. Klein Koerkamp et al. fabricated periodic arrays of subwavelength holes [21]. Schouten et al. fabricated a double slit structure [22]. These studies showed an extraordinary optical transmission with a normal incidence of light. In this study, we note the extraordinary optical transmission in double-layer WGPs and attempt to clarify this observation by the characterization of the polarization property of the double-layer WGP. This double-layer structure, as shown in Fig. 1a, is different from the abovementioned structures. These structures are composed of a metal layer and an electron beam (EB) resist layer. This study also characterized the dependence of transmission on the incident angle and clarified the relationship between transmission, incident angle, and the period observed for the double-layer WGPs.

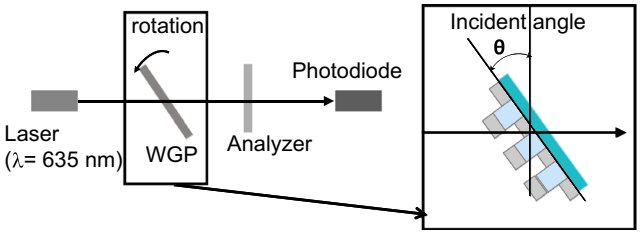

Fig. 2 Schematic of the experimental set-up for the measurement of transmittance

Experimental Methods

The double-layer WGP made on a glass substrate is fabricated by EBL (CABL-8000, CRESTEC) and DC magnetron sputtering (SC-701MC, SANYU). The line and space patterns are drawn using an EB resist (ZEP-520A, Zeon) on a glass substrate. Details on EBL are in [23]. After developing the resist layer, the Au layer is sputtered on the EB resist pattern. This double-layer WGP structure can be fabricated easier than the ordinal single-layer WGP because no lift-off process is required. The thickness of the EB resist is 100 nm and that of the Au layer is 40 nm. The period of the WGP (p) is varied between 200 and 1000 nm. The duty ratio of these line and space patterns is 0.5. The size of these samples was 1.5× 1.5 mm^2. The structures of the samples were observed by scanning electron microscopy (SEM) in the EBL. The schematics of the double-layer WGP are shown in Fig. 1a.

Polarization measurements were performed using a red laser diode with a wavelength λ=635 nm, as shown in Fig. 2. TE or TM polarized light is used to illuminate the fabricated sample. The incident angle can be changed by rotating the sample. The dependence of the transmittance of the double-layer WGP on incident angle was characterized for different periods by varying the incident angle from 0 to 70 deg. The 0th order transmitted light was detected by a photodiode.

Experimental Results

The structure of the fabricated WGP (Fig. 1a) was characterized using SEM. Figure 1b shows the surface morphology of the double-layer WGP, as observed using SEM. The period of

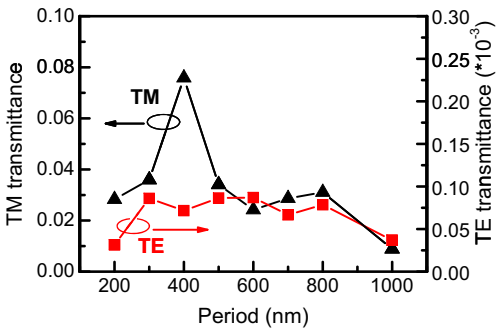

Fig. 3 Dependence on TE and TM transmittance of normal incidence on the period

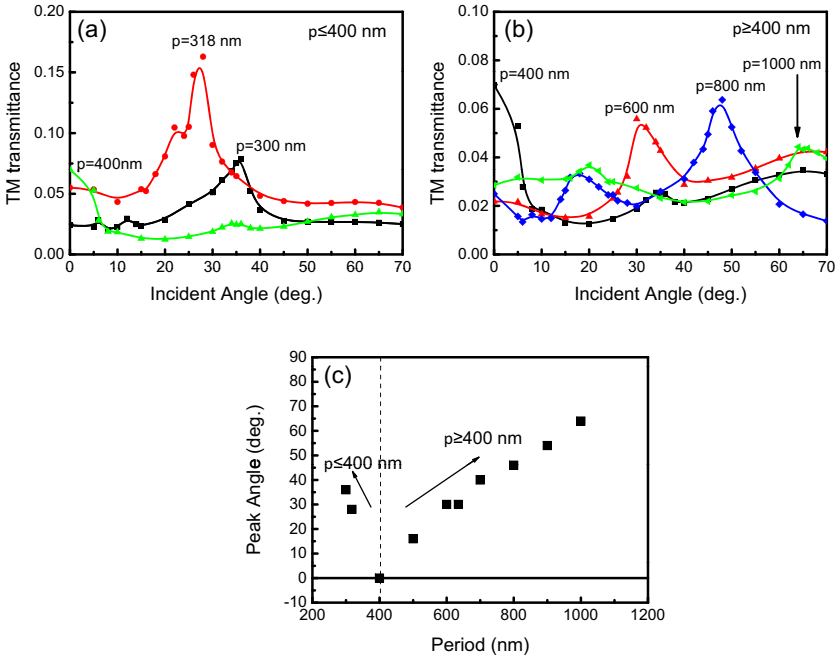

Fig. 4 Relationship between the period and incident angle, corresponding to the peak of TM transmittance (**a** p<400 nm, **b** p>400 nm) and relationship between the period and the peak angle (**c**)

this sample is 600 nm. From the depth profile obtained from AFM, the height is close to 100 nm.

The polarization property of the fabricated double-layer WGP was then characterized. TE and TM polarized light were used to illuminate the fabricated double-layer WGP, then the intensity of the transmitted light was measured by the photodiode. First, the TE and TM transmittance of normal incidence for various periods were characterized. Figure 3 shows the dependence of TE and TM transmittance of normal incidence on the period. The highest transmittance of TM polarization was obtained for a period of 400 nm. Conversely, the transmittance of TE polarization was about 1000 times smaller than that of TM polarization. The extinction ratio for the 400-nm period was 30.4 dB, which is almost the same as that of the commercial products. Subsequently, we characterized the dependence of TM transmittance on the incident angle. Figure 4 shows the relationship between the period and incident angle, corresponding to the peak of TM transmittance. In both cases of $p \leq 400$ nm (Fig. 4a) and $p \geq 400$ nm (Fig. 4b), when p is 400 nm, the peak angle is almost 0°. However, when p was smaller or larger than 400 nm, the peak angle varied with the period and shifted to the higher degree side. Conversely, TE transmittance was about 1000 times smaller than TM transmittance and was independent of the wavelength. For these experiments, the incident plane is perpendicular to the direction of the WGP; thus, TE transmittance is expected to be

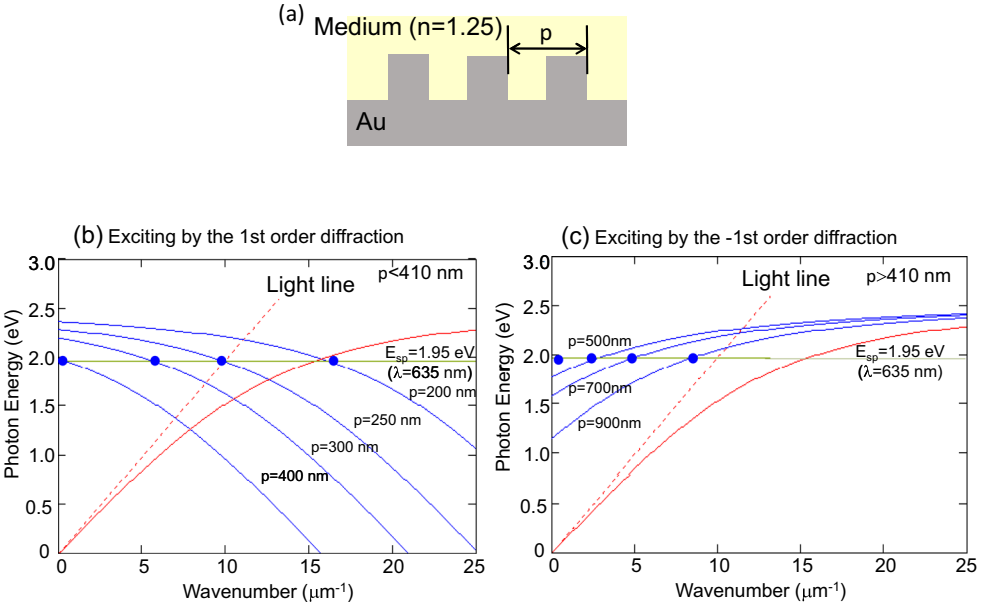

Fig. 5 Schematic of the model used for calculating the SPP dispersion curve (**a**) and dispersion curve of SPP for (**b**) p<410 nm and (**c**) p>410 nm

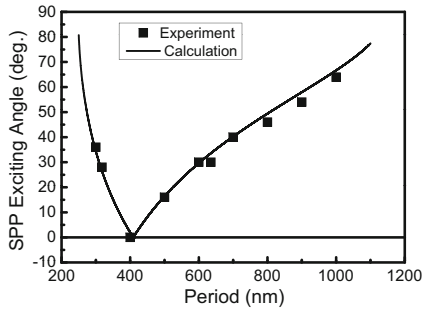

Fig. 6 Relationship between the period and incident angle, which shows a peak corresponding to the TM transmittance from the experimental data and calculated data

almost 0 and there are no relationships between transmittance and period like with TM transmittance. The extinction ratio at p=318 nm is 33.8 dB. The maximum extinction ratio is 45 dB for the research experiment [9] and 30–45 dB for commercial products. Our research data were close to those of commercial products. The relationship between the peak angle and the period of WGP is shown in Fig. 4c. When p is 400 nm, the peak angle is 0°. For the other period, the peak angle is shifted to higher angle.

Theoretical Results

To consider the peak shift of the incident angle, we first considered the interference between the reflection light from the top and bottom Au layer. However, this interference cannot be explained because there are no conditions for it at the wavelength (635 nm) and height (100 nm). Therefore, we speculated on the extraordinary optical transmission phenomena by surface plasmon resonance [20]. For the simplified model as shown in Fig. 5a, composed of an Au grating and with a dielectric medium of refractive index 1.25, which is the average of air and the resist, the dispersion relationship of the SPPs and the incident angle that excites the SPPs are calculated as follows. Given that the complex dielectric constant of a metal is $\varepsilon_1=\varepsilon_1'+i\varepsilon_1''$ and that of a dielectric is ε_2, the dispersion relation for SPPs at the metal–dielectric interface with incident angle θ exciting the SPPs are given by the following equations [24],

$$k_{sp}=\frac{\omega}{c}\sqrt{\frac{\varepsilon_1'\varepsilon_2}{\varepsilon_1'+\varepsilon_2}}+i\frac{\omega}{c}\left(\frac{\varepsilon_1'\varepsilon_2}{\varepsilon_1'+\varepsilon_2}\right)^{\frac{3}{2}}\frac{\varepsilon_1''}{2\varepsilon_1'^{2,}} \quad (1)$$

$$k\sin\theta=\frac{2\pi n\ \sin\theta}{\lambda_0}=\mathrm{Re}\{k_{sp}\}, \quad (2)$$

where k is the wavenumber of the incident light, k_{sp} is that of the SPP, c is the light velocity, ω is the angular frequency of the incident light, θ is the incident angle, n is the refractive index of the medium, and λ_0 is the wavelength of the incident light in the air.

Figure 5 shows the dispersion curve of SPPs for (b) p<410 nm and (c) P>410 nm. Figure 5b presents the SPP dispersion curve of Au films on the right side of the light line. This means that the SPPs cannot be excited on the Au film.

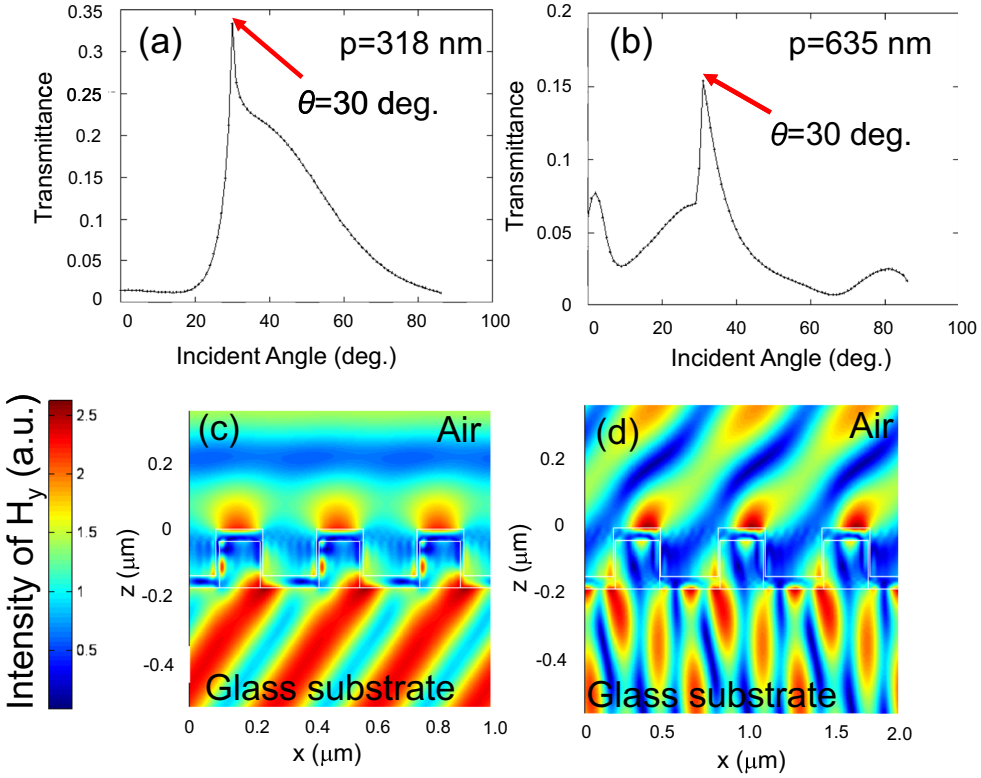

Fig. 7 Dependence of the 0th order transmission on the incident angle and the calculated magnetic field (**a** p=318 nm, **b** p=635 nm) and their distribution on the magnetic field (**c** p=318 nm, **d** p=635 nm)

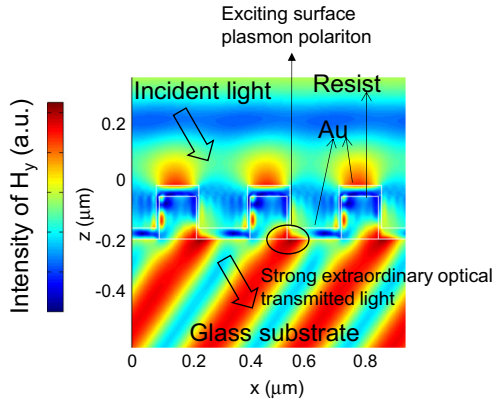

Fig. 8 Mechanism of the extraordinary optical transmission phenomena

However, for the grating structures, the 1st order diffraction contributes to the excitation of the SPPs. Figure 5c presents the −1st order diffraction contribution to excite the SPPs. In both figures, there are intersections between the dispersion curves and the light energy (1.95 eV, 635 nm). From these intersections, the incident angle exciting the SPPs can be obtained. Figure 6 shows the relationship between the period and incident angle, which shows a peak corresponding to the TM transmittance of experimental data and calculated data. The calculated data are almost identical to the experimental data. From this result, the peak shift is found related to the exciting SPP.

The distribution of the electrical field is calculated by the rigorous coupled-wave analysis method using commercial software (rcda-1d [Source Forage]). Figure 7 shows the dependence of the 0th order transmission on the incident angle and the calculated magnetic field. The peak angle is 30° (p=318 nm) and 30° (p=635 nm), as shown in Fig. 7a, b. When p is equal to 318 nm, the maximum calculated transmittance at 30° is 0.3. However, when p=635 nm, the maximum calculated transmittance at 30° is 0.3. The magnetic field distributions are shown in Fig. 7c, d. When the incident angle is the same as the peak angle, the TM light can be transmitted to the glass substrate. When p is equal to 316 nm, the incident TM light can be transmitted to the glass substrate and a strong magnitude of the magnetic field can be obtained. Notably, in the interface between Au and the glass substrate, the magnitude of the magnetic field is largest. It can be shown that only when the incident angle is identified with the exciting angle of surface plasmon polariton, the TM light can be transmitted to the glass substrate.

Discussion

The mechanism of the extraordinary optical transmission phenomena is explained in Fig. 8, which shows the distribution of magnetic field for a period of 318 nm and an incidence angle of 30°. From the experiments and dispersion curve, p=250–1000 nm are found as the exciting conditions of SPP. Our studies have yet to find the reason for obtaining maximum transmission. However it is considered that p=318 nm is half of the wavelength of the incident light. The magnetic field is concentrated at the interface of Au and the resist in the vicinity of the glass substrate. It is suggested that the incident light passes through the resist layer from its side wall, followed by the excitation of SPPs at the interface between the resist and Au. Subsequently, the SPPs combine with the transmitted light in the glass substrate. This results in strong transmitted light with TM polarization. In contrast to previous reports, where light with a normal incidence was used [20–22], in this study, the light is incident from an oblique angle. Therefore, it is considered extraordinary transmission is observed in these structures.

Conclusion

We clarified the relationship between the structural and polarization properties in a double-layer WGP to determine the optimal structure. The polarization property of the fabricated double-layer WGP for different periods was characterized with the incident angle varying from 0 to 70°. The peak incident angle of TM transmittance was found to vary as a function of the period. This can be explained on the basis of the extraordinary optical transmission phenomena by surface plasmons.

Acknowledgments This study is supported by the Nippon Sheet Glass Foundation for Materials Science and Engineering and JSPS KAKENHI (Grant Numbers 25600090, 26390082, 15H03556). The authors would like to thank Edanz for English language support.

Conflict of Interest The authors declare that they have no conflict of interest.

References

1. Bird GR, Parrish M Jr (1960) The wire grid as a near-infrared polarizer. J Opt Soc Am 50:886–891. doi:10.1364/JOSA.50.000886
2. Hass M, O'Hara M (1965) Sheet infrared transmission polarizers. Appl Opt 4:1027–1031. doi:10.1364/AO.4.001027
3. Auton JP (1967) Infrared transmission polarizers by photolithography. Appl Opt 6:1023–1027. doi:10.1364/AO.6.001023
4. Stenkamp B, Abraham M, Ehrfeld W, Knapek E, Hintermaier E, Gale MT, Morf R (1994) Grid polarizer for the visible spectral region. Proc SPIE 2213:288–296. doi:10.1117/12.180973
5. Lochbihler H, Depine R (1993) Highly conducting wire gratings in the resonance region. Appl Opt 32:3459–3465. doi:10.1364/AO.32.003459
6. Tamada H, Doumuki T, Yamaguchi T, Matsumoto S (1997) Al wire-grid polarizer using the s-polarization resonance effect at the 0.8-mm-wavelength band. Opt Lett 22:419–421. doi:10.1364/OL.22.000419

7. Yu XJ, Kwok HS (2003) Optical wire-grid polarizers at oblique angles of incidence. J Appl Phys 93:4407–4412. doi:10.1063/1.1559937
8. Xu M, Urbach HP, de Boer DKG, Cornelissen HJ (2005) Wire-grid diffraction gratings used as polarizing beam splitter for visible light and applied in liquid crystal on silicon. Opt Express 13:2303–2320. doi:10.1364/OPEX.13.002303
9. Wang JJ, Walters F, Liu X, Sciortino P, Deng X (2007) High-performance, large area, deep ultraviolet to infrared polarizers based on 40 nm line/78 nm space nanowire grids. Appl Phys Lett 90:061104. doi:10.1063/1.2437731
10. Hsu SY, Lee KL, Lin EH, Lee MC, Wei PK (2009) Giant birefringence induced by plasmonic nanoslit arrays. Appl Phys Lett 95:013105. doi:10.1063/1.3167772
11. Beresna M, Gecevičius M, Kazansky PG, Gertus T (2011) Radially polarized optical vortex converter created by femtosecond laser nanostructuring of glass. Appl Phys Lett 98:201101. doi:10.1063/1.3590716
12. Iwami K, Ishii M, Kuramochi Y, Ida K, Umeda N (2012) Ultrasmall radial polarizer array based on patterned plasmonic nanoslits. Appl Phys Lett 101:161119. doi:10.1063/1.4761943
13. Ishii M, Iwami K, Umeda N (2015) An Au nanofin array for high efficiency plasmonic optical retarders at visible wavelengths. Appl Phys Lett 106:021115. doi:10.1063/1.4905369
14. Djalalian-Assl A, Cadusch AA, Teo ZQ, Davis TJ, Roberts A (2015) Surface plasmon wave plates. Appl Phys Lett 106:041104. doi:10.1063/1.4906596
15. Yu Z, Deshpande P, Wu W, Wang J, Chou SY (2000) Reflective polarizer based on a stacked double-layer subwavelength metal grating structure fabricated using nanoimprint lithography. Appl Phys Lett 77:927–929. doi:10.1063/1.1288674
16. Ekinci Y, Solak HH, David C, Sigg H (2006) Bilayer Al wire-grids as broadband and high performance polarizers. Opt Express 14:2323–2334. doi:10.1364/OE.14.002323
17. Ye Z, Peng Y, Zhai T, Zhou Y, Liu D (2011) Surface plasmon-mediated transmission in double-layer metallic grating polarizers. J Opt Soc Am B 28:502–507. doi:10.1364/JOSAB.28.000502
18. Ye Z, Zheng J, Sun S, Chen S, Liu D (2013) Compact color filter and polarizer of bilayer metallic nanowire grating based on surface plasmon resonances. Plasmonics 8:555–559. doi:10.1007/s11468-012-9433-6
19. Ma Y, Sun N, Zhang R, Guo L, She Y, Zheng J, Ye Z (2014) Integrated color filter and polarizer based on two-dimensional superimposed nanowire arrays. J Appl Phys 116:044314. doi:10.1063/1.4891804
20. Ebbesen TW, Lezec HJ, Ghaemi HF, Thio T, Wolff PA (1998) Extraordinary optical transmission through sub-wavelength hole arrays. Nature 391:667–669. doi:10.1038/35570
21. Klein Koerkamp KJ, Enoch S, Segerink FB, van Hulst NF, Kuipers L (2004) Strong influence of hole shape on extraordinary transmission through periodic arrays of subwavelength holes. Phys Rev Lett 92:183901. doi:10.1103/PhysRevLett.92.183901
22. Schouten HF, Kuzmin N, Dubois G, Visser TG, Gbur G, Alkemade PFA, Blok H, 't Hooft GW, Lenstra D, Eliel G (2005) Plasmon-assisted two-slit transmission: Young's experiment revisited. Phys Rev Lett 94:053901. doi:10.1103/PhysRevLett.94.053901
23. Motogaito A, Hiramatsu K (2013) Fabrication of binary diffractive lenses and the application to LED lighting for controlling luminosity distribution. Opt Photon J 3:67–73. doi:10.4236/opj.2013.31011
24. Okamoto K, Kawakami Y (1999) High-efficiency InGaN/GaN light emitters based on nanophotonics and plasmonics. IEEE J Sel Top Quantum Electron 15:1199–1209. doi:10.1109/JSTQE.2009.2021530